Scientia Iranica D (2023) 30(1), 167–182

Sharif University of Technology
Scientia Iranica
Transactions D: Computer Science & Engineering and Electrical Engineering
http://scientiairanica.sharif.edu

Finite-time synchronization of a new five-dimensional hyper-chaotic system via terminal sliding mode control

J. Mostafaee[a], S. Mobayen[b,c,*], B. Vaseghi[d], and M. Vahedi[a]

a. *Department of Electrical Engineering, Saveh Branch, Islamic Azad University, Saveh, Iran.*
b. *Department of Electrical Engineering, University of Zanjan, Zanjan, Iran.*
c. *Future Technology Research Center, National Yunlin University of Science and Technology, 123 University Road, Section 3, Douliu, Yunlin 64002, Taiwan, R.O.C.*
d. *Department of Electrical Engineering, Abhar Branch, Islamic Azad University, Abhar, Iran.*

Received 1 July 2020; received in revised form 27 February 2021; accepted 31 May 2021

KEYWORDS
Hyper-chaotic system;
Chaos synchronization;
Terminal sliding mode control;
Finite-time stability;
Robustness.

Abstract. This study constructs a new 5D nonlinear hyper-chaotic system with attractive and complex behaviors. The standard behaviors of the chaotic system will also be analyzed including: Equilibrium Point (EP), Bifurcation Diagram (BD), Poincare Map (PM), Lyapunov Exponent (LE), and Kaplan-Yorke dimensional. We prove that the introduced new 5D hyper-chaotic system has complex and nonlinear behaviors. Next, the work describes Fast Terminal Sliding Mode Control (FTSMC) scheme for the control and finite-time fast synchronization of the novel 5D nonlinear hyper-chaotic system. Proof of stability for both phases has been done for the new controller with the Lyapunov stability theory. To ensure synchronization, both master-slave subsystems are perturbed by different parameter and model uncertainties. Both steps of the Sliding Mode Controller (SMC) have chaos-based fast convergence properties. Subsequently, it has been shown that the state paths of both master-slave systems can reach each other in a limited time. One of the features of the novel controller in this paper is high performance and finite-time stability of the terminal sliding surface due to derivative error and other errors. Finally, by using the MATLAB simulation, the results are confirmed for the new hyper-chaotic system.

1. Introduction

With the advent and development of telecommunication, especially wireless communications, encryption and information hiding has become a communication necessity [1]. With the progress of multimedia and communication technologies as well as the limitations of transportation, medical images have played an important role in tele-surgery. At the same time, new communication technologies have enabled medical image sharing and processing. These technologies have also increased security issues such as confidentiality and integrity [2]. Given these advantages, it is risky to send electronic patient records and medical confidential records to common networks such as the Internet. Although sending information to these networks is less expensive, it will have security risks, including the availability of information to everyone. Therefore, one of the necessities of information transfer, especially medical information, is increased security of information transfer [3]. In 1998, Friedrich introduced image encoding using a two-dimensional chaotic function.

*. *Corresponding author.*
E-mail addresses: mobayen@znu.ac.ir; mobayens@yuntech.edu.tw (S. Mobayen)

doi: 10.24200/sci.2021.56313.4657

Using the chaotic adaptive conversion method, he designed a novel idea for chaos-based image encryption based on random encryption [4].

Chaotic systems have a number of intrinsic properties, including high oscillations as well as complex nonlinear dynamical equations [5]. Two important features of chaotic systems are parametric uncertainty and sensitivity to change in their initial conditions. Chaos programs are now highly developed. Due to the unpredictability of these systems, they can be used in many applications including nonlinear anti-synchronization [6], chaos-based control [7], encryption [8], robotic [9], biological networks [10], secure communication [11], and neuroscience [12]. Many 3D nonlinear systems have been designed, among which the systems developed by Chen and Ueta [13], Lu and Chen [14], and Qi et al. [15] are generic. These systems, despite their good features, have one positive Lyapunov Exponent (LE) and a simple structure. As a result, these systems have a weak security flaw that makes them easy to break. Therefore, Rossler introduced a hyper-chaotic system with two or more LEs [16]. The hyper-chaotic systems have more nonlinear behaviors and higher fluctuations than the chaotic systems [6,17]. Many high-dimensional hyper-chaotic systems are designed based on the available low-dimensional nonlinear chaotic systems by two methods as follows:

- Feeding back the output of the nonlinear control into the chaos system equation characterized by low dimension [18];
- Junctioning two low-dimensional nonlinear chaos systems together [19].

One way to create a nonlinear hyper-chaotic system is to add the dimensions of a general chaotic system, leading to instability. Alternatively, a usual method is to get a novel nonlinear hyper-chaotic system via adding one or more other state variables to a regular nonlinear chaos system [20], e.g., the Chen and Ueta [13], Lorenz [21], Lü and Chen [14], and Qi systems [22]. In a chaos-based secure communication, the master-slave subsystems can be used to transmit a secure communication. When these two systems are synchronized, we will have a complete and successful transfer. The chaos-based synchronization is one of the main control approaches [23] has been considered by researchers for many years [24]. For a successful chaos-based synchronization, a suitable control signal is used to move the state trajectories of the two chaotic nonlinear subsystems. In recent years, several linear and nonlinear controllers including linear and nonlinear feedback control [25–27], adaptive tracking control [28,29], backstepping design [30], optimal nonlinear control [31,32], fuzzy controller [33], Proportional-Integral-Derivative (PID) control [34], stochastic control [35,36], active control [37], general Sliding Mode Controller (SMC) [38], linear feedback method [39], passive control [40], finite time stability [41,42], SMC [43], and Terminal Sliding Mode Control (TSMC) [44] have been utilized for chaos-based synchronization. Among these studies done based on control theories topics, most of them have investigated asymptotic synchronization.

Of all the stated methods, the SMC is characterized by such specifications as asymptotic stability, computational simplicity, simple implementation, parametric robustness, reduced order of the system, suitable transient response, and less sensitivity to bounded disturbance [45]. In this method, due to the linear sliding surface, the convergence time is unbounded and the system states reach the Equilibrium Point (EP) asymptotically [46]. Given the importance of time in the transmission of medical information, conditions must be provided to transfer the information as quickly as possible. Compared with the traditional SMC, the TSMC introduces a non-linear term in the sliding surface function to improve the convergence properties of the system to ensure that the system modes converge to a given trajectory in a limited time span [47].

Much research has been done over the years on the application and development of SMC design [48,49]. In [50], two Adaptive Sliding Mode Control (ASMC) approaches to synchronizing the Genesio-Tesi system with external disturbance and unknown parameters are proposed. In [51], using a Second-Order Sliding Mode Control (SOSMC), chaos-based synchronizations uncertain with different structures were investigated. With all the advantages and popularity of the SMC, this method has a major drawback called the chattering phenomenon. This phenomenon is very undesirable in practice and will have such effects as controller malfunction, mechanical wear in systems, and increased energy consumption. Much research has been done by researchers to solve this problem. For example, in [52], a new chatter-free SMC strategy with integral operators being differential was designed for synchronization and chaos control signal to the nonlinear uncertain chaos systems. In [53], using the chaotic system proposed in [54], a new controller for a chaos-based synchronization strategy was dedicated to fractional-order nonlinear systems characterized by several dimensions. It is shown that the error goes to zero in the bounded-time. In [55], a new fixed-time chattering-free observer-based SMC scheme was proposed for chaos-based synchronization of two-sided teleoperations under an unknown time-varying delay. Using an SMC scheme, this system was evaluated for unknown disturbances at a fixed time. The observer-based fixed-time SMC is designed to estimate the unmeasured speed state, while the position state is supposed to be available. In this paper, the fixed time stability method is used for convergence. A new SMC scheme is proposed to synchronize drive systems to response system in the presence of time-delay in the communication channel, as well as states and estimating disturbances. The authors in [56] investigated a novel robust predefined time chattering-free SMC strategy for the nonlinear tracking control problem of a Remotely Operated Vehicle (ROV) with Three-Degree Of Freedom (3-DOF) with uncertainties. Upon defining a novel sliding surface, a novel SMC scheme was designed to ease the chatter phenomenon and tracking precision without damaging the robustness properties. The results illustrated that the proposed control scheme could solve the design problem of the predefined time tracking controller and also provide robustness to various uncertainties. The Lyapunov stability theory is used at both sliding phase and the reaching phase. In [57], a novel nine-terms hyper-chaotic system with line equilibrium was first designed. This system enjoys rich behavior and attractors have been developed and all of the attractive features of the system have been analyzed. Finally, synchronization between two new 9D nonlinear systems using active control was designed. In [58], an SMC scheme was presented for nonlinear chaotic systems. The proposed new controller was built on a new SMC reaching law and a nonlinear sliding surface in the bounded time. In [59], a new robust controller was designed. The new control strategy was proposed for digital secure information between two nonlinear subsystems with unknown parameters and uncertainties within a finite time by TSMC and combining adaptive backstepping approaches. The TSMC provides faster convergence than the general SMC. In [60], two different new controllers were developed using Non-singular Terminal Sliding Mode Control (NTSMC) and the other Adaptive Non-singular Terminal Sliding Mode Control (ANTSMC) methods with unknown parameters and different uncertainties for synchronization. The concept of TSMC method ensures controller robustness against various external disturbances and parametric uncertainties and, also, guarantees system stability in a bounded time. Based on the above existing results, the master-master system is synchronized in an infinite time. However, some engineering problems created in different structures are expected to be synchronized in a bounded time. The chaos-based fast synchronization has many advantages and features, such as finite-time tracking, optimality of the convergence time, improved robustness, and rejection of uncertainties and disturbances.

For an unauthorized receiver, chaos-based decryption is difficult without knowing the dynamics of the system and the initial conditions. One of the secure ways is to increase the dynamic of the nonlinear chaotic system, because it is difficult to recover messages for unauthorized sources using retrieval methods. Another way to increase security is the dynamic complexity of the system, as this will make decoding difficult. For example, in [61], general chaos-based synchronization between two new integer-order and fractional-order hyper-chaotic nonlinear systems was studied. The new control signals were constructed using the technique of stability theory and the tracking controller of the fractional-order system. In [62], the chaos-based time-bound synchronization of the four-dimensional Memristor Chaos Systems (MCS) was studied. First, an emulator circuit of a memristor was created to implement the MCS. Then, based on the presented emulator circuit, the model of the MCS was provided and its time-bound chaotic synchronization is achieved under the designed new controller. Finally, sustainability analysis has been performed. In [63], chaos-based synchronization of nonlinear Lu systems with disturbance and uncertainty and minor control scheme with regard to systems' dimensions by applying an ASMC was presented. First, an Integral-Type Sliding Mode Control (I-TSMC) was proposed for chaos-based synchronization of nonlinear Lu systems upon specifying positive parameters. Second, a new control signal was used for synchronization of nonlinear master-slave Lu systems; in this case, unspecified positive parameters are estimated using an adaptive control rule. Finally, stability of the designed control scheme is proved using the Lyapunov stability method. In [64], ASMC method was proposed for chaos-based synchronization of 6D drive-response nonlinear systems in the presence of unknown parameters and external disturbance in the response system. First, two 6D integer-order drive-response systems in the presence of unknown parameters and external disturbance signal in the response system were designed. Second, after identifying chaos in fractional-order dynamic of the foresaid system, chaos-based synchronization of 6D nonlinear fractional-derivative drive-response systems in the presence of uncertainty, disturbance signal, and unknown parameters in the response system was studied, in which fractional-order Riemann-Liouville derivative was used. A novel sliding surface was defined for the new 6D nonlinear system to specify the proper active control. Finally, controller proofs and numerical simulations for the efficiency of the proposed design were presented in the presence of parametric uncertainty and disturbance.

Asymptotic stability is a weaker concept than finite-time stability. In finite-time stability, system state variables converge to their EP more rapidly in a finite time. The term "terminal" refers to the meaning of finite-time stability. Depending on the structure of the systems, there are many applications that need to be stable in a finite-time. The paper makes the following main contributions:

(i) Designing and building a 5-D hyper-chaotic system as well as analyzing and acquiring intrinsic properties;

(ii) Designing a novel Fast Terminal Sliding Mode Control (FTSMC) for the chaos-based synchronization of five-dimensional nonlinear master-slave systems;

(iii) Designing a new sliding surface and proving the global stability and fast convergence without chattering.

This article is as follows: Section 2 provides the general dynamical model of the novel 5D nonlinear system and its benefits and features. Then, the chaos-based fast synchronization problem of hyper-chaotic systems in a time-bound state is formulated. Section 3 presents the proof and design of the TSMC signal for chaos-based synchronization. Section 4 performs numerical simulations to prove the effectiveness of the methods. Section 5 presents some conclusions.

2. Problem definition and description

2.1. Model of the novel 5-D hyper-chaos system

The dynamics of the novel 5-D hyper-chaoatic system is described as:

$$\frac{dx_1(\tau)}{d\tau} = a_1(x_2 - x_1) - a_2x_5,$$

$$\frac{dx_2(\tau)}{d\tau} = a_3x_1 - x_2 - a_4x_4 - x_1x_3,$$

$$\frac{dx_3(\tau)}{d\tau} = -a_5x_3 + x_1x_2 + x_1^2,$$

$$\frac{dx_4(\tau)}{d\tau} = a_6x_5 + x_2,$$

$$\frac{dx_5(\tau)}{d\tau} = a_7x_2 + x_1, \tag{1}$$

where $a_i, (i = 1, ..., 7)$, $x_i, (i = 1, ..., 5)$, and τ are the constant positive parameters, state variables, and time of the new nonlinear system (1), respectively. The nonlinear system (1) will have hyper-chaotic behaviors by defining the following parameters:

$$a_1 = 8.83, \quad a_2 = 0.75, \quad a_3 = 36.36, \quad a_4 = 20.779,$$

$$a_5 = 7.79, \quad a_6 = 4.1, \quad a_7 = 4.286.$$

2.2. Dynamical behaviors and basic properties of the novel 5D nonlinear system

This section presents the general properties of Nonlinear System (1) such as: EP, chaotic attractors, eigen values, Kaplan-Yorke dimension, LE, Poincare Map (PM), and Bifurcation Diagram (BD). Upon setting the differential equations in new Nonlinear System (1) to zero, it is concluded that the 5D nonlinear system (1) has EP at: $Q = (0, 0, 0, 0, 0)$. The 5D nonlinear system linearization matrix [65] at the EP Q is given by:

$$J = \frac{\partial F_i}{\partial x_j}(x)\bigg|_{Q^*} = \begin{bmatrix} -a_1 & a_1 & 0 & 0 & -a_2 \\ a_3 & -1 & 0 & -a_4 & 0 \\ 0 & 0 & -a_5 & 0 & 0 \\ 0 & 1 & 0 & 0 & a_6 \\ 1 & a_7 & 0 & 0 & 0 \end{bmatrix}. \tag{2}$$

According to Linearization Matrix (2), the system eigenvalues are found as $p(s) = |sI_d - J| = 0$ with I_d as an 5×5 identity matrix, that is:

$$(s + a_5)[s^4 + A_1s^3 + A_2s^2 + A_3s + A_4],$$

$$A_1 = (a_1 - a_1a_3 + 1),$$

$$A_2 = (a_1 - a_1a_3a_5 + a_4a_6a_7 + a_2a_3a_7),$$

$$A_3 = (a_1a_4a_6a_7 + a_4a_5a_6a_7 + a_2a_3a_5a_7 + a_1a_4a_6 + a_2a_4),$$

$$A_4 = (a_1a_4a_5a_6a_7 + a_1a_4a_5a_6 + a_2a_4a_5). \tag{3}$$

By using parameter values in System (1), the eigenvalues are:

$$s_1 = -23.2488, \; s_2 = 8.7260, \; s_3 = 7.3648,$$

$$s_4 = -7.79, \; s_5 = -2.6719.$$

Thus, Q is an unstable saddle. The divergence of the nonlinear system (Eq. (1)) is as follows:

$$\nabla V = \sum_{i=1}^{5} \frac{\partial \dot{x}_i}{\partial x_i} = -a_1 - 1 - a_5 = -8.83 - 1 - 7.79 = -17.62 < 0. \tag{4}$$

Thus, the convergence speed of System (1) to its attractors is $e^{-(a_1-1-a_5)\tau}$. The phase portrait diagrams of System (1) are depicted in Figures 1 and 2. The convergence and divergence of the states of the nonlinear systems are specified by its LE representation. If LEs are positive, it indicates the chaos and hyper-chaotic behaviors of the nonlinear system [66,67]. The LEs of the novel 5-D nonlinear system (Eq. (1)) with initial conditions $(x_1(0) = -1.2)$, $(x_2(0) = 3.8)$, $(x_3(0) = 7.7)$, $(x_4(0) = 2.7)$, $(x_5(0) = 1.4)$, are numerically determined as $LE_1 = 2.512$, $LE_2 = 0.211$, $LE_3 = -2.155$, $LE_4 = -4.286$, $LE_5 = -13.89$, shown in Figures 3 and 4. According to the numerical values obtained for LEs, the Kaplan-Yorke dimensional [68,69] of the 5D nonlinear system (Eq. (1)) is defined as: $D_{KY} = 4.7115$, which is fractional. The BDs examine

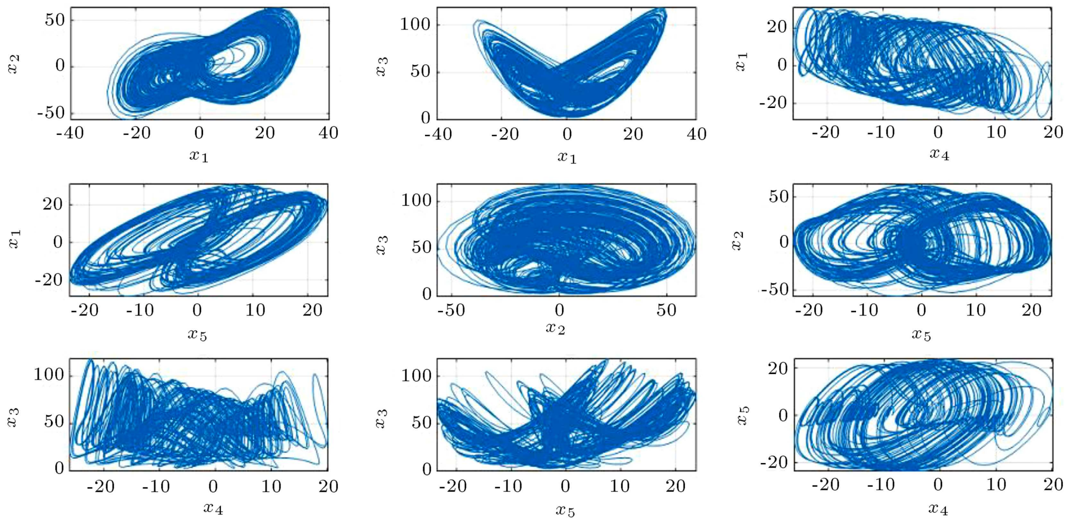

Figure 1. $x - y$ plane of the five-dimensional nonlinear system (Eq. (1)).

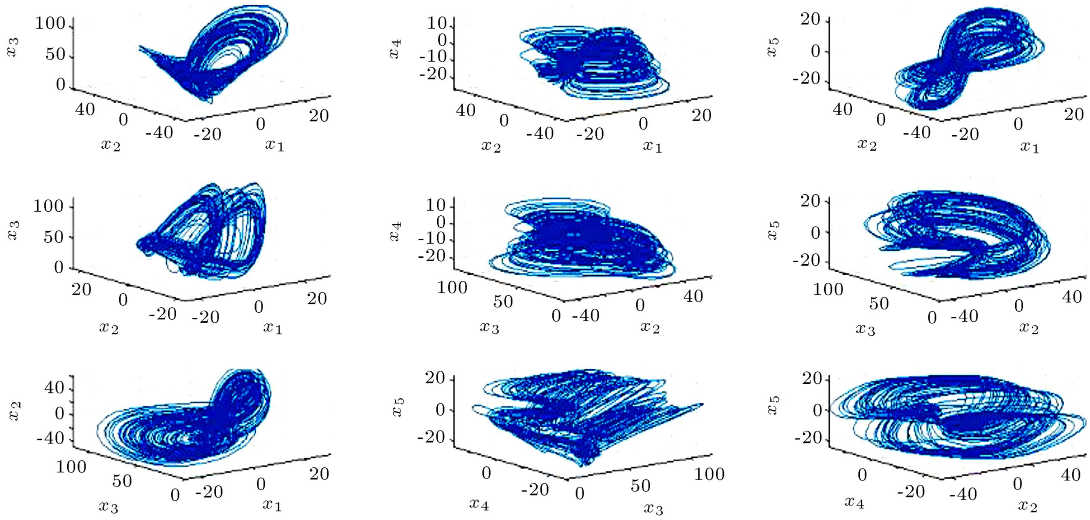

Figure 2. $x - y - z$ plane of the five-dimensional nonlinear system (Eq. (1)).

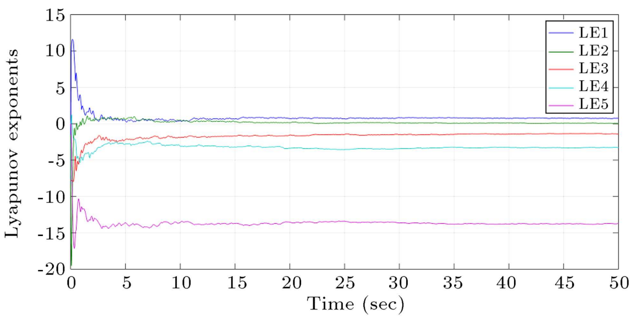

Figure 3. Dynamics of Lyapunov Exponent (LE) of the five-dimensional nonlinear system (Eq. (1)).

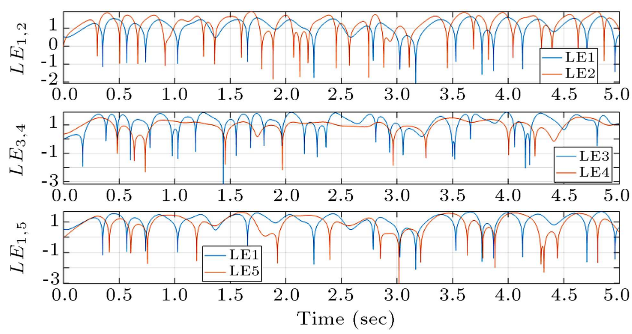

Figure 4. Lyapunov Exponent (LE) spectrum of the nonlinear system (Eq. (1)).

the dependence of the parameter values of the chaos nonlinear systems. In Figure 5, BDs of Nonlinear System (1) are plotted. Nonlinear System (1) enters into chaotic oscillations with routine period doubling [70,71]. Another attraction of chaotic nonlinear systems is the use of PMs to describe the folding properties of the system. This method is one of the most famous topics in the nonlinear dynamical analysis that we can use to prove the behavior and performance of continuous dynamic systems similar to the proposed

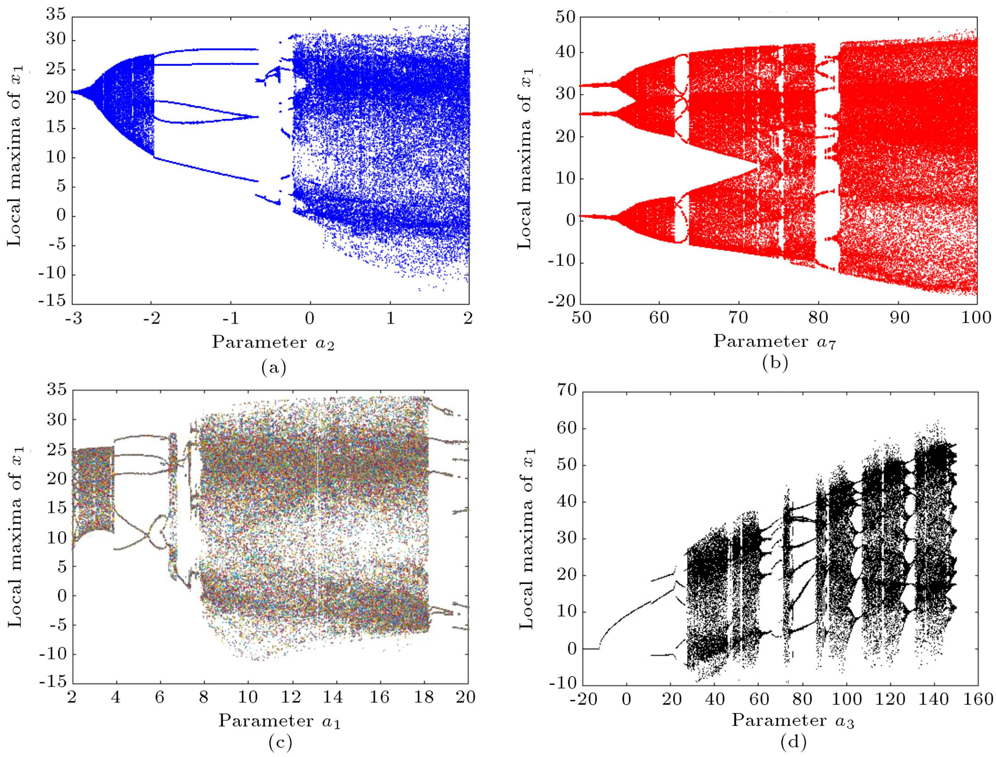

Figure 5. Bifurcation Diagram (BD) of the five-dimensional nonlinear system (Eq. (1)) in (a) (a_2, x_1), $a_2 \in (-3, 2)$, (b) (a_7, x_1), $a_7 \in (50, 100)$, (c) (a_1, x_1), $a_1 \in (2, 20)$, and (d) (a_3, x_1), $a_3 \in (-20, 150)$.

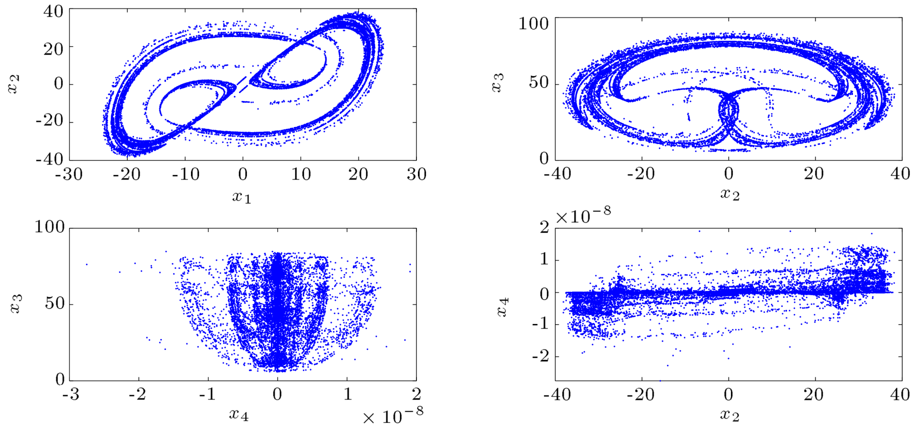

Figure 6. Poincare Map (PM) of the five-dimensional nonlinear system (Eq. (1)) in (a) $x_1 - x_2$ map, (b) $x_2 - x_3$ map, (c) $x_4 - x_3$ map, and (d) $x_2 - x_4$ map.

5D nonlinear system (1). Figure 6 displays the PMs of 5D Nonlinear System (1). According to Figure 6, the regular set of points represents the chaotic behavior of the system.

2.3. Problem formulation

In this section, chaos-based fast synchronization is presented between two novel 5D nonlinear master-slave subsystems with homogeneous parametric uncertainties and unknown disturbances. Next, we use Nonlinear System (1) with changes in parameters and initial conditions to build master-slave subsystems for chaos-based synchronization. Consider the 5D nonlinear master system as follows:

$$\frac{dx_{im}(\tau)}{d\tau} = \begin{bmatrix} -a_1 & a_1 & 0 & 0 & -a_{2m} \\ a_{3m} + x_{3m} & -1 & 0 & -a_{4m} & 0 \\ x_{1m} + x_{2m} & 0 & -a_{5m} & 0 & 0 \\ 0 & 1 & 0 & 0 & a_{6m} \\ 1 & a_{7m} & 0 & 0 & 0 \end{bmatrix} x_{im} \quad (5)$$

where $a_{1m}, \cdots, a_{7m}$ and $X_m = x_{1m}, ..., x_{5m}$ are the parameters and states of Subsystem (5), respectively.

Thus, for the 5D nonlinear slave subsystem, we define:

$$\frac{dx_{is}(\tau)}{d\tau} = \begin{bmatrix} -a_1 & a_1 & 0 & 0 & -a_{2s} \\ a_{3s}+x_{3s} & -1 & 0 & -a_{4s} & 0 \\ x_{1s}+x_{2s} & 0 & -a_5 & 0 & 0 \\ 0 & 10 & 0 & a_{6s} & \\ 1 & a_{7s} & 0 & 0 & 0 \end{bmatrix}$$

$$x_{is} + \Lambda v(\tau) + d(\tau), \tag{6}$$

where $X_s = x_{1s}, ..., x_{5s}$ are the state variables of Subsystem (6) and $v(\tau) = v_1, ..., v_5$ are the nonlinear command signals used for synchronization of master-slave Subsystems (5) and (6).

Assumption 1: Let the chaos-based synchronization errors of Subsystems (5) and (6) be as follows: $e_i = x_{is} - x_{im} (i = 1, ..., 5)$.

Assumption 2: Constraints on uncertainties and disturbances are defined as follows:

$$|f(x(\tau))| \leq \iota_1, |d(\tau)| \leq \iota_2, \tag{7}$$

where ι_1 and ι_2 denote positive unknown constants.

Assumption 3: Suppose that $y_i(\tau) = x_i(\tau)$ implies that $\lim_{\tau\to\infty} e_i(\tau) = 0$.

Definition 1 [72]: The chaos-based synchronization of Subsystems (5) and (6) is obtained in a time-bound manner if $\lim_{\tau\to T} ||e(\iota)|| = 0$ and $||e(\iota)|| = 0$ for $\tau \geq$ T, where $T = T(e(\iota_0)) > 0$, $e(\iota) = [e_i]^T$ $(i = 1, ..., 5)$.

Definition 2 [73]: Hyper-chaotic master-slave Subsystems (5) and (6) are fast synchronization, if there is a control signal $v_p(\tau)$ and a constant $T > 0$ such that $\lim_{\tau\to T}[z_p^1(\tau) - z_p^2(\tau)] = 0$, where $z_p^1(\tau) - z_p^2(\tau)$ for $\tau > T, z^1(\tau)$ and $z^2(\tau)$ are the solutions of 5D hyper-chaotic master-slave Subsystems (5) and (6).

Lemma 1 [11]: If the $\vartheta(\tau)$ is a positive definite performance such that:

$$\dot{\vartheta}(\tau) \leq -\delta\vartheta^\theta(\tau), \quad \forall\tau \geq \tau_0, \quad \vartheta(\tau_0) \geq 0, \tag{8}$$

where $\delta > 0$, $0 < \theta < 1$ are constants and known for any initial time τ_0, then, function $\vartheta(\tau)$ satisfies:

$$\vartheta^{1-\theta}(\tau) \leq \vartheta^{1-\theta}(\tau_0) - \delta(1-\theta)(\tau - \tau_0), \ \tau_0 \leq \tau \leq \tau_1, \tag{9}$$

and:

$$\vartheta(\tau) \equiv 0, \quad \forall\tau \geq \tau_1, \tag{10}$$

with the settling time τ_1 satisfying:

$$\tau_1 \leq \tau_0 + \frac{\vartheta^{1-\theta}(\tau_0)}{\delta(1-\theta)}. \tag{11}$$

Lemma 2: Suppose that the function $\nu(\tau)$, which is continuous and positive definite, satisfies the following equation [74]:

$$\dot{\nu}(\tau) \leq -\alpha\nu(\tau) - \beta\,\nu^\eta(\tau) \quad \forall\tau \geq \tau_0, \quad \nu(\tau_0) \geq 0. \tag{12}$$

At all times τ_0, the function $\nu(\tau)$ at the finite time τ_s will converge to zero. Thus, we have:

$$\tau_s = \tau_0 + \frac{1}{\alpha(1-\eta)} \ln \frac{\alpha\,\nu^{1-\eta}(\tau_0) + \beta}{\beta}. \tag{13}$$

3. Main results

Consider the dynamical model as:

$$\dot{x}(\tau) = \Lambda x(\tau) + Bv(\tau) + f(x(\tau)) + d(\tau), \tag{14}$$

where $x(\tau)$ is state variables, B and Λ are the constant matrices, $v(\tau)$ is the controller, $f(x(\tau))$ is the nonlinear functions of the nonlinear first-order system (14) and $d(\tau)$ sum of the unknown disturbance and uncertainty of Nonlinear System (14). The sliding surface for System (14) is defined as:

$$l(\tau) = Gx(\tau), \tag{15}$$

where G is the gain coefficient (row vector) as $G = [\wp_1, \wp_2, \wp_3, \wp_4, \wp_5]$.

In order to satisfy the issue that $l(\tau)$ converges to origin in the finite time, the following fast terminal sliding surface is given as:

$$s(\tau) = \dot{l}(\tau) + \lambda l(\tau) + \mu l^\eta(\tau), \tag{16}$$

where λ, μ, and η the positive constant values and ratio of two odd positive integers with $1 > \eta > 0$, respectively.

Theorem 1: Let the FTSMC for Nonlinear System (14) be defined as:

$$\begin{aligned}\dot{v}(\tau) = &-(GB)^{-1}\Big\{\left(\lambda + \mu\eta l(\tau)^{\eta-1}\right) \\ &G\left[\Lambda x(\tau) + f(x(\tau)) + Bv(\tau)\right] \\ &+ G\left(\Lambda^2 x(\tau) + \Lambda f(x(\tau)) + \Lambda Bv(\tau) + \dot{f}(x(\tau))\right) \\ &+ \kappa|s(\tau)|^\eta + \gamma s(\tau) + \chi \mathrm{sgn}(s(\tau))\Big\},\end{aligned} \tag{17}$$

where κ and γ are optional positive constants and χ satisfies:

$$\chi \geq \max\left[\left(\left(\lambda + \mu\eta l(\tau)^{\eta-1}\right) G + G\Lambda\right) d(\tau) + G\dot{d}(\tau)\right]. \tag{18}$$

With the control scheme (Eq. (17)), the state trajectories of the nonlinear dynamic system (Eq. (14)) move to the sliding surface (Eq. (15)) in finite time and they stay there.

Assumption 4: Function $f(x(\tau)) \in R^{n\times 1}$ satisfies the following conditions:

$$\forall x \in R^{n\times 1}, |f(x(\tau))| \neq 0. \tag{19}$$

Assumption 5: GB is a non-singular (invertible) matrix.

Assumption 6: System (14) tracking errors reach origin in a limited time span using the control scheme (Eq. (17)).

Proof: We follow the steps of the finite-time stability of the FTSMC at two phases as follows:

(a) Reaching phase: Considering the sliding surface Eq. (16), the Lyapunov candidate function can be considered as follows:

$$v_1(\tau) = 0.5\zeta s^2(\tau). \tag{20}$$

Lemma 3 [75]: The following inequalities are established:

$$\left|\sum_1^\infty \frac{\psi(1+\xi)}{\psi(1+\kappa)\psi(1-\kappa+\xi)} D^k s \mathrm{D}^{\xi-k} s\right| \leq \delta|s|, \tag{21}$$

where δ is a positive constant. In Eq. (20), ζ is equal to:

$$\sum_1^\infty \frac{\psi(1+\xi)}{\psi(1+k)\psi(1-k+\xi)} s\dot{s}. \tag{22}$$

Differentiating the Lyapunov function (Eq. (22)) yields:

$$\begin{aligned}\dot{\nu}_1(\tau) =& s(\tau)\dot{s}(\tau) \\ &+ \sum_1^\infty \frac{\psi(1+\xi)}{\psi(1-k+\xi)\psi(1+k)} s(\tau)\dot{s}(\tau) \\ &\leq s(\tau)\dot{s}(\tau) + \left|\sum_1^\infty \frac{\psi(1+\xi)}{\psi(1-k+\xi)\psi(1+k)}\right. \\ &\left. s(\tau)\dot{s}(\tau)\right|. \end{aligned} \tag{23}$$

According to Eq. (21), we yield:

$$\begin{aligned}\dot{\nu}_1(\tau) \leq& s(\tau)\dot{s}(\tau) \\ &+ \left|\sum_1^\infty \frac{\psi(1+\xi)}{\psi(1+k)\psi(1-k+\xi)} s(\tau)\dot{s}(\tau)\right| \\ &\leq s(\tau)\dot{s}(\tau) + \delta|s(\tau)|. \end{aligned} \tag{24}$$

By substituting Eq. (16) into Eq. (24), we have:

$$\dot{\nu}_1(\tau) \leq s(\tau)\frac{d}{d\tau}(\dot{l}(\tau) + \lambda l(\tau) + \mu l^\eta(\tau)) + \delta|s(\tau)|. \tag{25}$$

By substituting Eq. (14) into Eq. (25), we have:

$$\begin{aligned}\dot{\nu}_1(\tau) \leq& s(\tau)\frac{d}{d\tau}\Big((G\Lambda x(\tau) + GBv(\tau) + Gf(x(\tau)) \\ &+ Gd(\tau)) + \lambda Gx(\tau) + \mu(Gx(\tau))^\eta\Big) + \delta|s(\tau)| \\ &= s(\tau)\Big((G\Lambda \dot{x}(\tau) + GB\dot{v}(\tau) \\ &+ G\dot{f}(x(\tau)) + G\dot{d}(\tau)) + \lambda G\dot{x}(\tau) \\ &+ \mu(G\dot{x}(\tau))^\eta\Big) + \delta|s(\tau)| \leq |s(\tau)|\Big|G\Lambda\dot{x}(\tau) \\ &+ G\dot{d}(\tau) + \lambda G\dot{x}(\tau) + \mu(G\dot{x}(\tau))^\eta\Big| \\ &+ \Big(s(\tau) + G\dot{f}(x(\tau)) + GB\dot{v}(\tau)\Big) + \delta|s(\tau)|. \end{aligned} \tag{26}$$

Assumption 7: The uncertainty disturbances are considered bounded as follows:

$$|\frac{d^\alpha}{d\tau}(d_i(\tau))| \leq \gamma, \tag{27}$$

where γ is a positive custom constant.

Assumption 8: Assume that the sign function is bounded as:

$$\left|\frac{d^\alpha}{d\tau}\rho_i \mathrm{sgn}(\mu x_i)\right| \leq \kappa, \tag{28}$$

where κ is a positive constant. Using Eqs. (17) and (26), we can write Eq. (29) as shown in Box I. According to Assumptions 7 and 8, using Eqs. (18) and (26), we obtain:

$$\begin{aligned}\dot{\nu}_1(\tau) \leq& |s(\tau)|\Big(\Big|G\Lambda\dot{x}(\tau) + G\dot{d}(\tau) + \lambda G\dot{x}(\tau) \\ &+ \mu(G\dot{x}(\tau))^\eta\Big| - \kappa - \gamma\Big) + |s(\tau)| \\ &(-G - \chi\,|\mathrm{sgn}(s(\tau))| - \kappa|s(\tau)|^\eta) + \delta|s(\tau)|. \end{aligned} \tag{30}$$

From Eqs. (27) and (28), one gets:

$$\dot{\nu}_1(\tau) \leq -(G + |\chi \mathrm{sgn}(s(\tau))| - \delta)\,|s(\tau)| - \kappa s(\tau)^{\eta+1}, \tag{31}$$

Therefore, we have:

$$\dot{\nu}_1(\tau) \leq -(G-\delta)\,|s(\tau)| = -\Theta|s(\tau)|. \tag{32}$$

Therefore, the state trajectories of the first-order nonlinear system (Eq. (14)) will converge to the sliding surface $s(\tau) = 0$ with $G > \delta$.

With the designed reaching law (Eq. (32)), switching function will reach the sliding surface in finite time

$$\dot{\nu}_1(\tau) \leq |s(\tau)| \left| G\Lambda\dot{x}(\tau) + G\dot{d}(\tau) + \lambda G\dot{x}(\tau) + \mu(G\dot{x}(\tau))^{\eta} \right|$$
$$+s(\tau)\left[G\dot{f}(x(\tau)) - \left[\begin{array}{l} (\lambda + \mu\eta l(\tau)^{\eta-1}) \\ \quad G[\Lambda x(\tau) + Bv(\tau) + f(x(\tau))] \\ +\kappa|s(\tau)|^{\eta} + G(\Lambda^2 x(\tau) \\ \quad +\Lambda Bv(\tau) + \Lambda f(x(\tau)) + \dot{f}(x(\tau))) \\ \quad +\gamma s(\tau) + \chi \mathrm{sgn}(s(\tau)) + \delta|s(\tau)| \end{array} \right] \right]. \tag{29}$$

Box I

τ_s with proper positive constant G and the stability-time is defined as:

$$\tau_s = \{\inf \tau \geq \tau_r : \mathrm{X}_i(\tau) = 0\}, \tag{33}$$

where τ_r is the time to reach the EP.

By integrating from Eq. (32) from 0 to τ_r, one gets:

$$v_1(\tau_r) - {v_1}^{\zeta-1}(0)\frac{{\tau_r}^{\zeta-1}}{\Psi(\zeta)} \leq -(G-\delta)\frac{d^{-\zeta}}{d\tau}|s(\tau)|. \tag{34}$$

Assuming that $\frac{d^{-\zeta}}{d\tau}|s(\tau)| \geq \Gamma$ is bounded and $v_1(\tau_r) = 0$, we will have:

$${v_1}^{\zeta-1}(0)\frac{{\tau_r}^{\zeta-1}}{\Psi(\zeta)} \leq -(G-\delta)\Gamma. \tag{35}$$

Therefore, we have:

$$\tau_r \leq \left(\frac{{v_1}^{\zeta-1}(0)}{(G-\delta)\Gamma}\right)^{1/1-\zeta}. \tag{36}$$

(b) Sliding phase: Considering the sliding surface (Eq. (16)), the Lyapunov candidate function can be considered as follows:

$$V(\tau) = 0.5s(\tau)^2. \tag{37}$$

From Eq. (16), the time-derivative of the FTSMC surface is found as:

$$\dot{s}(\tau) = \ddot{l}(\tau) + \left(\lambda + \mu\eta l(\tau)^{\eta-1}\right)\dot{l}(\tau), \tag{38}$$

where using Eqs. (14) and (15), we have:

$$\begin{aligned}\dot{s}(\tau) &= G\ddot{x}(\tau) + \left(\lambda + \mu\eta l(\tau)^{\eta-1}\right)G\dot{x}(\tau) \\ &= G\left(\Lambda\dot{x}(\tau) + B\dot{v}(\tau) + \dot{f}(x(\tau)) + \dot{d}(\tau)\right) \\ &\quad + \left(\lambda + \mu\eta l(\tau)^{\eta-1}\right)G\dot{x}(\tau) \\ &= G\Big(\Lambda^2 x(\tau) + \Lambda f(x(\tau)) + \Lambda Bv(\tau) + \Lambda d(\tau) \\ &\quad + \dot{f}(x(\tau)) + B\dot{v}(\tau) + \dot{d}(\tau)\Big) \\ &\quad + \left(\lambda + \mu\eta l(\tau)^{\eta-1}\right)G[\Lambda x(\tau) \\ &\quad + Bv(\tau) + f(x(\tau)) + d(\tau)].\end{aligned} \tag{39}$$

Differentiating the Lyapunov function (Eq. (37)) and using Eq. (39) yields:

$$\begin{aligned}\dot{V}(\tau) = s(\tau)\Big\{ &\left(\lambda + \mu\eta l(\tau)^{\eta-1}\right) \\ &G\left[\Lambda x(\tau) + f(x(\tau)) + d(\tau) + Bv(\tau)\right] \\ &+ G\Big(\Lambda^2 x(\tau) + \Lambda f(x(\tau)) + \Lambda d(\tau) \\ &+ \Lambda Bv(\tau) + B\dot{v}(\tau) + \dot{f}(x(\tau)) + \dot{d}(\tau)\Big)\Big\},\end{aligned} \tag{40}$$

where substituting Eq. (17) into Eq. (40) yields:

$$\begin{aligned}\dot{V}(\tau) =& -\kappa|s(\tau)|^{\eta+1} - \gamma s(\tau)^2 - \chi s(\tau)\mathrm{sgn}(s(\tau)) \\ &+ s(\tau)\Big(\Big(\left(\lambda + \mu\eta l(\tau)^{\eta-1}\right)G + G\Lambda\Big)d(\tau) \\ &+ G\dot{d}(\tau)\Big) \leq -\kappa|s(\tau)|^{\eta+1} - \gamma s(\tau)^2 - \chi|s(\tau)| \\ &+ |s(\tau)|\Big|\Big(\left(\lambda + \mu\eta l(\tau)^{\eta-1}\right)G + G\Lambda\Big)d(\tau) \\ &+ G\dot{d}(\tau)\Big|.\end{aligned} \tag{41}$$

Using Eqs. (18) and (41), we can write as follows:

$$\begin{aligned}\dot{V}(\tau) &\leq -\gamma|s(\tau)|^2 - \kappa|s(\tau)|^{\eta+1} \\ &= -\alpha V(\tau) - \beta V^{\bar{\eta}}(\tau),\end{aligned} \tag{42}$$

where $\bar{\eta} = (\eta+1)/2 < 1$, $\alpha = 2\gamma > 0$, and $\beta = 2^{\bar{\eta}}\kappa >$

0. Thus, the value of Lyapunov's function (Eq. (37)) decreases and the sliding surface converges to the origin in a finite time. Therefore, the proof is complete.

4. Simulation results

This section constructs a chaos-based fast synchronization between the 5D nonlinear master-slave subsystems with parametric uncertainty and unknown disturbances. All numerical simulations were performed using Simulink MATLAB software and with a solver of ode45 and step size of 0.001. Here, both 5D nonlinear master-slave subsystems (Eqs. (5) and (6)) for fast synchronization were used. Figure 7 displays the amazing 5D nonlinear attractor of the master subsystem (5) with initial condition $x_{1m}(0) = -1.19$, $x_{2m}(0) = 3.8$, $x_{3m}(0) = 7.7$, $x_{4m}(0) = 2.7$, $x_{5m}(0) = 1.4$ and parameters $a_{1m} = 8.84$, $a_{2m} = 0.76$, $a_{3m} = 36.4$, $a_{4m} = 20.82$, $a_{5m} = 7.78$, $a_{6m} = 4.09$, and $a_{7m} = 4.28$. Similarly, the amazing 5D nonlinear attractors of the slave subsystem (Eq. (6)) with initial condition: $x_{1s}(0) = 1.19$, $x_{2s}(0) = 4$, $x_{3s}(0) = -1.5$, $x_{4s}(0) = 3.8$, $x_{5s}(0) = -0.75$ and parameters $a_{1s} = 8.83$, $a_{2s} = 0.75$, $a_{3s} = 36.36$, $a_{4s} = 20.779$, $a_{5s} = 7.79$, $a_{6s} = 4.1$, $a_{7s} = 4.286$, are shown in Figure 8. According to Assumption 2, total uncertainties and disturbances are added to the slave subsystem given by Eq. (6).

We consider the hyper-chaotic systems (Eqs. (5) and (6)) with different initial conditions and unequal parameters for fast synchronization. According to As-

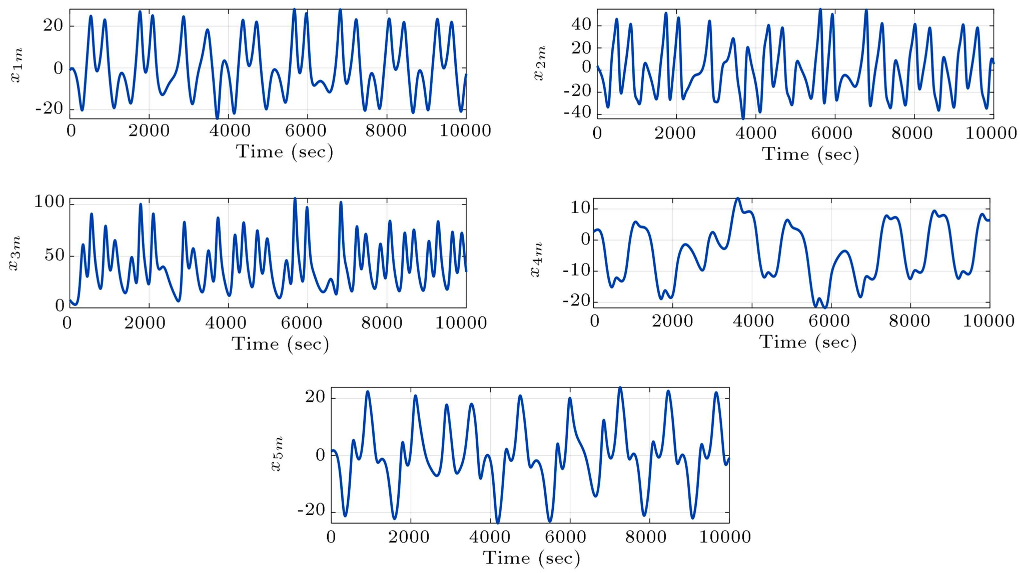

Figure 7. Five-dimensional nonlinear time trajectories of Subsystem (5).

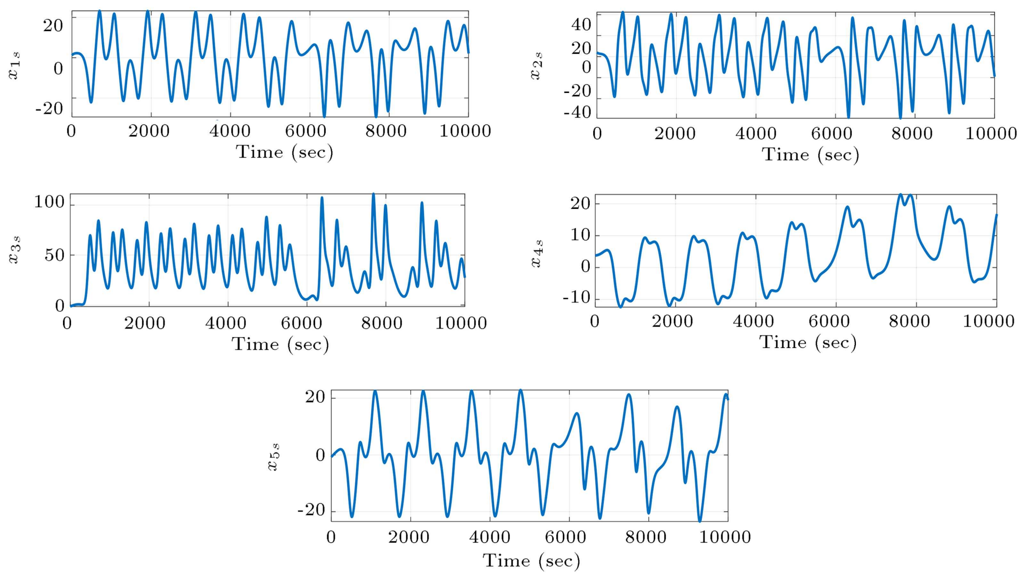

Figure 8. Five-dimensional nonlinear time trajectories of Subsystem (6).

sumption 1, to prove chaos-based fast synchronization, according to Subsystems (5) and (6), the errors can be designed as follows:

$$e_i = \sum_{i=1}^{5} y_i - x_i \Rightarrow$$

$$\begin{cases} \dot{e}_1 = -a_1e_1 + a_1e_2 - a_2e_5 \\ \dot{e}_2 = a_3e_1 - e_2 - a_4e_4 - y_1y_3 + x_1x_3 \\ \dot{e}_3 = -a_5e_3 + y_1y_2 - x_1x_2 + y_1^2 - x_1^2 \\ \dot{e}_4 = a_6e_5 + e_2 \\ \dot{e}_5 = a_7e_2 + e_1 \end{cases}$$

$$+ \begin{bmatrix} b_1 \\ b_2 \\ b_3 \\ b_4 \\ b_5 \end{bmatrix} \upsilon(\tau) + \begin{bmatrix} d_1 \\ d_2 \\ d_3 \\ d_4 \\ d_5 \end{bmatrix}. \tag{43}$$

System (43) in the matrix form is:

$$\frac{de_i(\tau)}{d\tau} = \Lambda e_i(\tau) + f(e(\tau)) + B\upsilon(\tau) + D(\tau), \tag{44}$$

where:

$$e = \begin{bmatrix} e_1 \\ e_2 \\ e_3 \\ e_4 \\ e_5 \end{bmatrix}, \qquad B = \begin{bmatrix} 0 \\ 1 \\ 1 \\ 0 \\ 1 \end{bmatrix},$$

$$f(e(\tau)) = \begin{bmatrix} 0 \\ x_{1s}x_{3s} - x_{1m}x_{3m} \\ -x_{1s}x_{2s} + x_{1m}x_{2m} - x_{1s}^2 + x_{1m}^2 \\ 0 \\ 0 \end{bmatrix},$$

$$A = \begin{bmatrix} -8.83 & 8.83 & 0 & 0 & -0.75 \\ 36.36 & -1 & 0 & -20.779 & 0 \\ 0 & 0 & -7.79 & 0 & 0 \\ 0 & 1 & 0 & 0 & 4.1 \\ 1 & 4.286 & 0 & 0 & 0 \end{bmatrix},$$

$$D(\tau) = random\ number. \tag{45}$$

Then, according to Theorem 1, chaos-based fast synchronization between two subsystems Eq. (5) and (6) with error equation (Eq. (44)) is definite in a finite time. Therefore, we use the new control signal (Eq. (17)) for synchronization and select the positive control gains in the new controller (Eq. (17)) as follows:

$$G = (85, 5, 0.05, 3795, 2096). \tag{46}$$

The $d(\tau)$ and $f(\tau)$ functions are specified in Eq. (45). The sliding surface (Eq. (16)) parameters are $\lambda = 10$, $\mu = 50$, and $\eta = \frac{1}{19}$. Using the control signal (Eq. (17)) with $\kappa = 20$, and $\gamma = 30$, we are sure we will have chaos-based synchronization in a finite time. Figure 9 displays the complete chaos-based fast synchronization of the master-slave subsystems (Eqs. (5) and (6)). According to Eq. (45) in the initial conditions, the errors of finite-time fast synchronization without the controller are shown in Figure 10. By applying the control scheme (Eq. (17)), the errors of finite-time fast synchronization obtained are the same as those depicted in Figure 11. Finally, the control input used for the synchronization is shown in Figure 12. It is shown that no chattering phenomenon exists in the control input. According to the simulation results, it is easy to observe that the 5D nonlinear master-slave subsystems (Eqs. (5) and (6)) are synchronized in a finite time. Figure 13 shows the time series of chaos-based fast synchronization errors designed in this

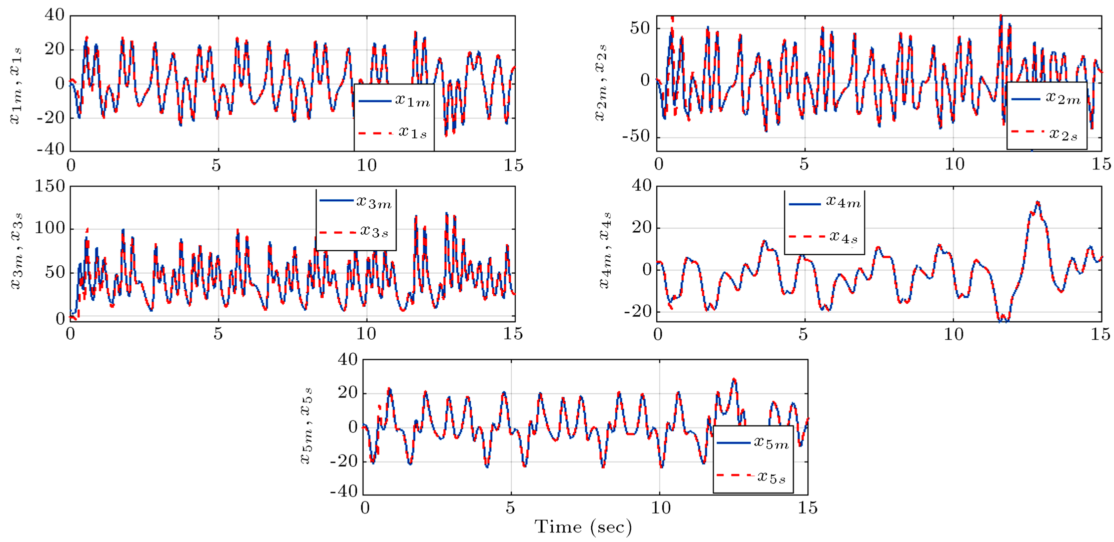

Figure 9. Chaos-based synchronization between two master-slave subsystems.

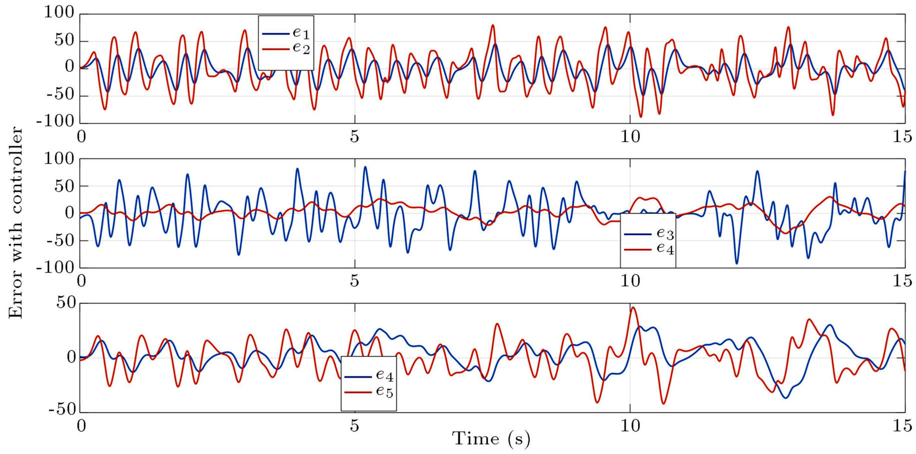

Figure 10. The errors of fast synchronization without the controller.

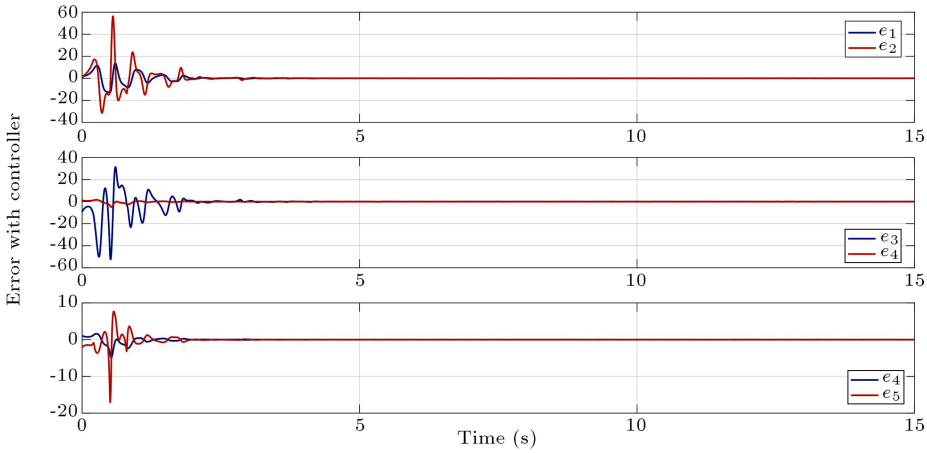

Figure 11. The errors of fast synchronization with the controller.

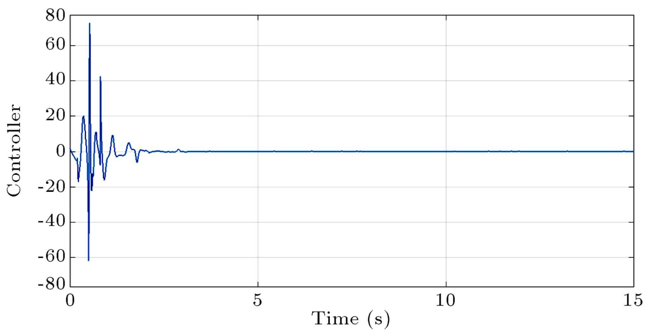

Figure 12. Simulation results of the input control during fast synchronization.

paper with the same controller. As is known, the designed controller (Eq. (17)) has better results than the controller designed in [7]. Moreover, it is obvious from this figure that the designed control method produces low overshoot and better settling time.

5. Conclusions

A new five-dimensional hyper-chaotic system was reported in this study. The dynamical behaviors of the new system were analyzed using time series trajectories, phase portraits, Poincare Map (PM), Lyapunov Exponent (LE), Bifurcation Diagram (BD), and Kaplan-Yorke dimension. The new 5D nonlinear system had an extremely complicated structure and dynamics. Next, a Fast Terminal Sliding Mode Control (FTSMC) was designed for stabilizing the new nonlinear system with disturbances and uncertainty. The main weakness of FTSMC is that it encounters singularity drawback, which causes a complex value and a high control effort. A new controller was designed for finite-time synchronization between the two identical proposed 5D nonlinear master-slave subsystems in the presence of matched disturbances, different initial conditions, and unequal parameters. The novel terminal sliding surface can supply a particular convergence characteristic. Finally, the numerical simulations pointed to the viability of the designed methods. The simulations demonstrated that the analytical results and computational results were similar.

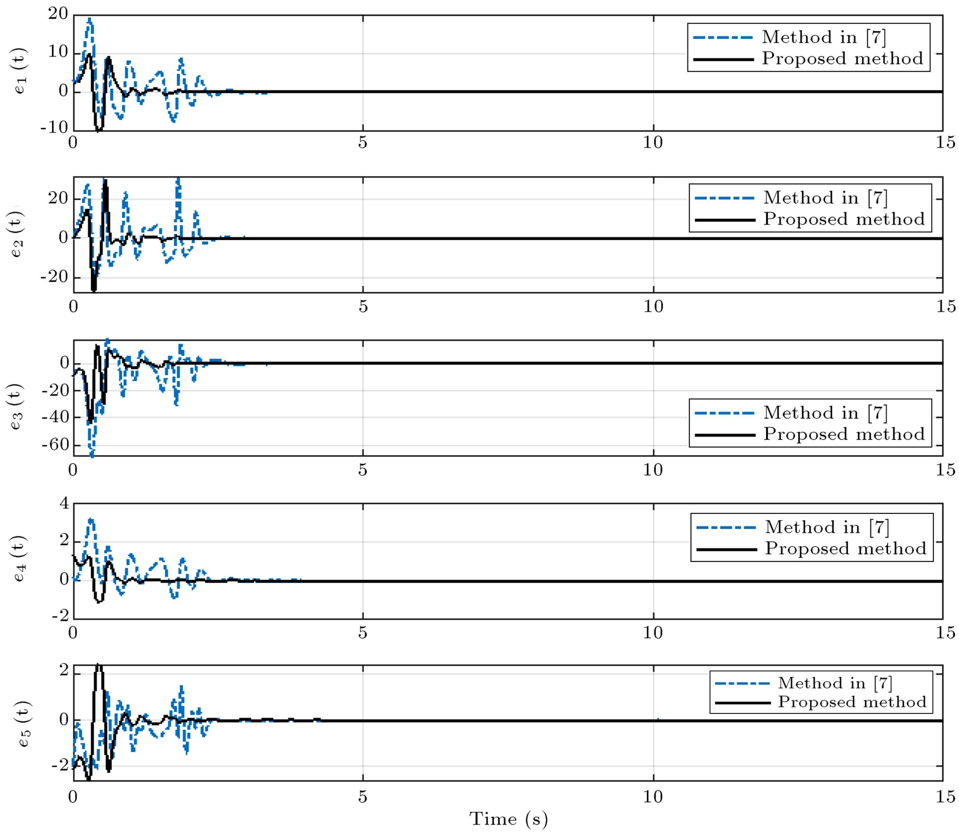

Figure 13. Time-response of the chaos-based fast synchronization errors.

References

1. Vaseghi, B., Pourmina, M.A., and Mobayen, S. "Secure communication in wireless sensor networks based on chaos synchronization using adaptive sliding mode control", *Nonlinear Dynamics*, **89**(3), pp. 1689–1704 (2017).

2. Coatrieux, G., Matre, H., Sankur, B., et al. "Relevance of watermarking in medical imaging", *International Conference on Information Technology Applications in Biomedicine*, IEEE, pp. 250–255 (2000).

3. Bouslimi, D., Coatrieux, G., and Roux, C. "A joint encryption/watermarking algorithm for verifying the reliability of medical images: Application to echographic images", *Computer Methods and Programs in Biomedicine.*, **106**(1), pp. 47–54 (2012).

4. Fridrich, J. "Symmetric ciphers based on two-dimensional chaotic maps", *International Journal of Bifurcation and Chaos.*, **8**(06), pp. 1259–1284 (1998).

5. Pai, M.C. "Chaos control of uncertain time-delay chaotic systems with input dead-zone nonlinearity", *Complexity*, **21**(3), pp. 13–20 (2012).

6. Al-sawalha, M.M. and Al-Dababseh, A.F. "Nonlinear anti-synchronization of two Hyper chaotic systems", *Applied Mathematical Sciences*, **5**(38), pp. 1849–1856 (2011).

7. Zhou, X., Wang, W., Liu, Z., et al. "Impact angle constrained three-dimensional integrated guidance and control based on fractional integral terminal sliding mode control", *IEEE Access*, **7**, pp. 126857–126870 (2019).

8. Hoang, T.M. "A chaos-based Image cryptosystem using nonstationary dynamics of logistic map", *International Conference on Information and Communication Technology Convergence (ICTC)*, IEEE, pp. 591–596 (2019).

9. Tlelo-Cuautle, E., Ramos-López, H.C., Sánchez-Sánchez, M., et al. "Application of a chaotic oscillator in an autonomous mobile robot", *Journal of Electrical Engineering*, **65**(3), pp. 157–162 (2014).

10. Minati, L., Ito, H., Perinelli, A., et al. "Connectivity influences on nonlinear dynamics in weakly-synchronized networks: Insights from Rössler Systems, Electronic Chaotic Oscillators, Model and Biological Neurons", *IEEE Access*, **7**, pp. 174793–174821 (2019).

11. Bao, H. and Cao, J. "Finite-time generalized synchronization of nonidentical delayed chaotic systems", *Nonlinear Analysis: Modelling and Control*, **21**(3), pp. 306–324 (2016).

12. Huang, Y. and Yang, X.-S. "Hyperchaos and bifurcation in a new class of four-dimensional Hopfield neural networks", *Neurocomputing*, **69**(13–15), pp. 1787–1795 (2006).

13. Chen, G. and Ueta, T. "Yet another chaotic attractor", *International Journal of Bifurcation and Chaos*, **9**(07), pp. 1465–1466 (1999).

14. Lü, J. and Chen, G. "A new chaotic attractor coined", *International Journal of Bifurcation and Chaos*, **12**(03), pp. 659–661 (2002).

15. Qi, G., Chen, G., Du, S., et al. "Analysis of a new chaotic system", *Physica A: Statistical Mechanics and its Applications*, **352**(2–4), pp. 295–308 (2005).

16. Rossler, O. "An equation for hyperchaos", *Physics Letters A.*, **71**(2–3), pp. 155–157 (1979).

17. Dimassi, H. and Loría, A. "Adaptive unknown-input observers-based synchronization of chaotic systems for telecommunication", *IEEE Transactions on Circuits and Systems I: Regular Papers*, **58**(4), pp. 800–812 (2010).

18. Gao, T., Chen, Z., Yuan, Z., et al. "A hyperchaos generated from Chen's system", *International Journal of Modern Physics C.*, **17**(04), pp. 471–478 (2006).

19. Yanchuk, S. and Kapitaniak, T. "Chaos-hyperchaos transition in coupled Rössler systems", *Physics Letters A*, **290**(3–4), pp. 139–144 (2001).

20. Barboza, R. "Dynamics of a hyperchaotic Lorenz system", *International Journal of Bifurcation and Chaos*, **17**(12), pp. 4285–4294 (2007).

21. Lorenz, E.N. "Deterministic nonperiodic flow", *Journal of the Atmospheric Sciences.*, **20**(2), pp. 130–141 (1963).

22. Qi, G. and Liang, X. "Force analysis of Qi chaotic system", *International Journal of Bifurcation and Chaos*, **26**(14), p. 1650237 (2016).

23. Jalnine, A.Y. "Generalized synchronization of identical chaotic systems on the route from an independent dynamics to the complete synchrony", *Regular and Chaotic Dynamics*, **18**(3), pp. 214–225 (2013).

24. Gonchenko, A.S., Gonchenko, S.V., and Kazakov, A.O. "Richness of chaotic dynamics in nonholonomic models of a Celtic stone", *Regular and Chaotic Dynamics*, **18**(5), pp. 521–538 (2013).

25. Tian, X., Yang, Z., and Fei, S. "Adaptive synchronization of fractional order chaotic systems based on modified feedback approach", *37th Chinese Control Conference (CCC)*, IEEE, pp. 10121–10126 (2018).

26. Canyelles-Pericas, P., Dai, X., Binns, R., et al. "Decomposing chaos into a harmonic oscillator with nonlinear feedback using pole placement methods", *56th Annual Conference on Decision and Control (CDC)*, IEEE, pp. 2078–2082 (2017).

27. Yang, C., Xiong, Z., and Yang, T. "Finite-time synchronization of coupled inertial memristive neural networks with mixed delays via nonlinear feedback control", *Neural Processing Letters*, **12**, pp. 1–18 (2020).

28. Meng, Z., Xia, Z., Yu, H., et al. "Neural adaptive synchronization control of chaotic FitzHugh-Nagumo neurons in the external electrical stimulation", *Chinese Control Conference (CCC)*, IEEE, pp. 2731–2736 (2019).

29. Tan, F., Zhou, L., Chu, Y., et al. "Fixed-time stochastic outer synchronization in double-layered multi-weighted coupling networks with adaptive chattering-free control", *Neurocomputing*, **29**, pp. 18–35 (2020).

30. Singh, P.P., Singh, J.P., and Roy, B. "Tracking control and synchronization of Bhalekar-Gejji chaotic systems using active backstepping control", *International Conference on Industrial Technology (ICIT)*, IEEE, pp. 322–326 (2018).

31. Liu, Z. "Design of nonlinear optimal control for chaotic synchronization of coupled stochastic neural networks via Hamilton–Jacobi–Bellman equation", *Neural Networks*, **99**, pp. 166–177 (2018).

32. Nguyen, V., Johnson, J., and Melkote, S. "Active vibration suppression in robotic milling using optimal control", *International Journal of Machine Tools and Manufacture*, **152**, p. 103541 (2020).

33. Wang, Y. and Yu, H. "Fuzzy synchronization of chaotic systems via intermittent control", *Chaos, Solitons & Fractals*, **106**, pp. 154–160 (2018).

34. Yau, H.-T., Wu, C.-H., Liang, Q.-C., et al. "Implementation of optimal PID control for chaos synchronization by FPGA chip", *International Conference on Fluid Power and Mechatronics* IEEE, pp. 56–61 (2011).

35. Chen, Y., Zhang, X., Shi, G., et al. "Synchronization of chaotic delayed neural networks via sampled-data feedback control with stochastic sampling", *Recent Advances in Computer Science and Information Engineering*, **28**, pp. 217–222 (2012).

36. Wu, J. and Li, X. "Global stochastic synchronization of kuramoto-oscillator networks with distributed control", *IEEE Transactions on Cybernetics*, **135**, pp. 1–11 (2020).

37. Henein, M.M., Sayed, W.S., Radwan, A.G., et al. "Switched active control synchronization of three fractional order chaotic systems", *International Conference on Electrical Engineering/Electronics, Computer, Telecommunications and Information Technology (ECTI-CON)*, IEEE, pp. 1–6 (2016).

38. Li, X.F. "Synchronization of chaotic permanent magnet synchronous motor system via sliding mode control", *International Conference on Systems Engineering (ICSEng)*, IEEE, pp. 1–4 (2018).

39. Tirandaz, H., Aminabadi, S.S., and Tavakoli, H. "Chaos synchronization and parameter identification of a finance chaotic system with unknown parameters, a linear feedback controller", *Alexandria Engineering Journal*, **57**(3), pp. 1519–1524 (2018).

40. Wu, X., Zhu, C., and Kan, H. "An improved secure communication scheme based passive synchronization of hyperchaotic complex nonlinear system", *Applied Mathematics and Computation*, **252**, pp. 201–214 (2015).

41. Sun, K., Zhu, S., Wei, Y., et al. "Finite-time synchronization of memristor-based complex-valued neural networks with time delays", *Physics Letters A.*, **383**(19), pp. 2255–2263 (2019).

42. Liu, X. "Adaptive finite time stability of delayed systems with applications to network synchronization", Available: arXiv:2002.00145 (2020).

43. Yan, J.-J., Yang, Y.-S., Chiang, T.-Y., et al. "Robust synchronization of unified chaotic systems via sliding mode control", *Chaos, Solitons & Fractals*, **34**(3), pp. 947–954 (2007).

44. Yin, L., Deng, Z., Huo, B., et al. "Finite-time synchronization for chaotic gyros systems with terminal sliding mode control", *IEEE Transactions on Systems*, **49**(6), pp. 1131–1140 (2017).

45. Mobayen, S. and Javadi, S. "Disturbance observer and finite-time tracker design of disturbed third-order nonholonomic systems using terminal sliding mode", *Journal of Vibration and Control*, **23**(2), pp. 181–189 (2017).

46. Slotine, J.-J.E. and Li, W. "Applied nonlinear control", *Prentice Hall Englewood Cliffs.*, pp. 1–461, New Jersey, US (1991).

47. Feng, Y., Zhou, M., Han, F., et al. "Speed control of induction motor servo drives using terminal sliding-mode controller", *Advances in Variable Structure Systems*, **36**, pp. 341–356 (2018).

48. Pisano, A. and Usai, E. "Output-feedback control of an underwater vehicle prototype by higher-order sliding modes", *Automatica*, **40**(9), pp. 1525–1531 (2004).

49. Besnard, L., Shtessel, Y.B., and Landrum, B. "Quadrotor vehicle control via sliding mode controller driven by sliding mode disturbance observer", *Journal of the Franklin Institute*, **349**(2), pp. 658–684 (2012).

50. Ghamati, M. and Balochian, S. "Design of adaptive sliding mode control for synchronization Genesio-Tesi chaotic system", *Chaos, Solitons & Fractals*, **75**, pp. 111–117 (2015).

51. Lü, L., Yu, M., and Luan, L. "Synchronization between uncertain chaotic systems with a diverse structure based on a second-order sliding mode control", *Nonlinear Dynamics*, **70**(3), pp. 1861–1865 (2012).

52. Li, H., Liao, X., Li, C., et al. "Chaos control and synchronization via a novel chatter free sliding mode control strategy", *Neurocomputing*, **74**(17), pp. 3212–3222 (2011).

53. Ouannas, A., Grassi, G., and Azar, A.T. "A new generalized synchronization scheme to control fractional chaotic systems with non-identical dimensions and different orders", *International Conference on Advanced Machine Learning Technologies and Applications*, Springer, pp. 415–424 (2019).

54. Wu, X., Wang, H., and Lu, H. "Modified generalized projective synchronization of a new fractional-order hyperchaotic system and its application to secure communication", *Nonlinear Analysis: Real World Applications*, **13**(3), pp. 1441–1450 (2012).

55. Abadi, A.S.S., Hosseinabadi, P.A., Mekhilef, S., et al. "Chattering-free fixed-time sliding mode control for bilateral teleoperation under unknown time-varying delay via disturbance and state observers", *Advanced Control for Applications: Engineering and Industrial Systems*, **2**(4), p. e52 (2020).

56. Hosseinabadi, P.A., Abadi, A.S.S., Mekhilef, S., et al. "Chattering-free trajectory tracking robust predefined-time sliding mode control for a remotely operated vehicle", *Journal of Control, Automation and Electrical Systems*, **31**, pp. 1–19 (2020).

57. Benkouider, K., Bouden, T., and Halimi, M. "Dynamical analysis, synchronization and circuit implementation of a new hyperchaotic system with line equilibrium", *International Conference on Control, Decision and Information Technologies (CoDIT)*, IEEE, pp. 1717–1722 (2019).

58. Lin, S. and Zhang, W. "Chattering reduced sliding mode control for a class of chaotic systems", *Nonlinear Dynamics*, **93**(4), pp. 2273–2282 (2018).

59. Zirkohi, M.M. "An efficient approach for digital secure communication using adaptive backstepping fast terminal sliding mode control", *Computers & Electrical Engineering*, **76**, pp. 311–322 (2019).

60. Abadi, A.S.S., Hosseinabadi, P.A., and Mekhilef, S. "Two novel approaches of NTSMC and ANTSMC synchronization for smart grid chaotic systems", *Technology and Economics of Smart Grids and Sustainable Energy*, **3**(1), p. 14 (2018).

61. Khan, A., Singh, S., Azar, A.T., et al. "Synchronization between a novel integer-order hyperchaotic system and a fractional-order hyperchaotic system using tracking control", *International Conference on Modelling, Identification and Control (ICMIC)*, IEEE, pp. 1–8 (2018).

62. Wang, L., Dong, T., and Ge, M.-F. "Finite-time synchronization of memristor chaotic systems and its application in image encryption", *Applied Mathematics and Computation*, **347**, pp. 293–305 (2019).

63. Sabaghian, A. and Balochian, S. "Parameter estimation and synchronization of hyper chaotic Lu system with disturbance input and uncertainty using two under-actuated control signals", *Transactions of the Institute of Measurement and Control*, **41**(6), pp. 1729–1739 (2019).

64. Sabaghian, A., Balochian, S., and Yaghoobi, M. "Synchronisation of 6D hyper-chaotic system with unknown parameters in the presence of disturbance and parametric uncertainty with unknown bounds", *Connection Science*, **32**(4), pp. 362–383 (2020).

65. Wiggins, S. "Introduction to applied nonlinear dynamical systems and chaos", *Springer Science & Business Media*, pp. 1–842, College Park, MD (2003).

66. Wolf, A., Swift, J.B., Swinney, H.L., et al. "Determining Lyapunov exponents from a time series", *Physica D: Nonlinear Phenomena.*, **16**(3), pp. 285–317 (1985).

67. Li, C., Gong, Z., Qian, D., et al. "On the bound of the Lyapunov exponents for the fractional differential systems", *Chaos: An Interdisciplinary Journal of Nonlinear Science*, **20**(1), p. 013127 (2010).

68. Grassberger, P. and Procaccia, I. "Characterization of strange attractors", *Physical Review Letters*, **50**(5), p. 346 (1983).

69. Grassberger, P. and Procaccia, I. "Measuring the strangeness of strange attractors", *Physica D: Nonlinear Phenomena*, **9**(1–2), pp. 189–208 (1983).

70. Mahmoud, E.E. "Generation and suppression of a new hyperchaotic nonlinear model with complex variables", *Applied Mathematical Modelling*, **38**(17–18), pp. 4445–4459 (2014).

71. Mahmoud, E.E. "Dynamics and synchronization of new hyperchaotic complex Lorenz system", *Mathematical and Computer Modelling*, **55**(7–8), pp. 1951–1962 (2012).

72. Yang, X. and Cao, J. "Finite-time stochastic synchronization of complex networks", *Applied Mathematical Modelling*, **34**(11), pp. 3631–3641 (2010).

73. Abdurahman, A., Jiang, H., and Teng, Z. "Finite-time synchronization for memristor-based neural networks with time-varying delays", *Neural Networks*, **69**, pp. 20–28 (2015).

74. Moulay, E. and Perruquetti, W. "Finite time stability and stabilization of a class of continuous systems", *Journal of Mathematical Analysis and Applications*, **323**(2), pp. 1430–1443 (2006).

75. Efe, M.Ö. "Fractional fuzzy adaptive sliding-mode control of a 2-DOF direct-drive robot arm", *IEEE Transactions on Systems*, **38**(6), pp. 1561–1570 (2008).

Biographies

Javad Mostafaee was born in Abyek, Qazvin, Iran in December 1982. He is currently working toward the PhD degree in Electrical Control Engineering at IAU, Saveh Branch, Iran. He is focusing on implementation and development of chaos-based control schemes. His research interests include image encryption, tracking control, nonlinear analysis, and chaos-based control and hyper-chaos systems.

Saleh Mobayen received the BSc and MSc degrees in Control and System Engineering from the University of Tabriz, Tabriz, Iran in 2007 and 2009, respectively, and received his PhD in Control and System Engineering from Tarbiat Modares University, Tehran, Iran in January 2013. From February 2013 to December 2018, he was as an Assistant Professor and a faculty member at the Department of Electrical Engineering of University of Zanjan, Zanjan, Iran. Since December 2018, he is an Associate Professor of Control and System Engineering at the University of Zanjan. He is the Associate Editor of various scientific journals. His research interests include nonlinear control, robust control, chaos theory, and robotic manipulators.

Behrouz Vaseghi was born in Esfahan, Iran in 1981. Since 2009, he has been an academic member of the Department of Electrical Engineering, Islamic Azad University, Abhar Branch, Iran. Since 2017, he has been an Assistant Professor at the Department of Electrical Engineering, Islamic Azad University, Abhar Branch. His research interests include video and audio processing, communication systems, chaos cryptography, chaotic systems, and chaos-based synchronization.

Mohammad Vahedi is an Assistant Professor at IAU of Saveh branch in Iran. Mohammad is now the Head of the Department of Mechanical Engineering at the Faculty of Engineering at IAU of Saveh in Iran. His research interests are robotic, vibration and control, robust control, and finite element method. He has published many papers in the area of sliding mode control, control and vibration, optimal control, and finite element method in various journals and conferences.